Ain Shams Engineering Journal 15 (2024) 102793

Contents lists available at ScienceDirect

Ain Shams Engineering Journal

journal homepage: www.sciencedirect.com

Full Length Article

Experimental study of phase change material (PCM) based spiral heat sink for the cooling process of electronic equipment

Yu Wang [a,*], Dheyaa J. Jasim [b], S. Mohammad Sajadi [c], Ghassan Fadhil Smaisim [d,e], Salema K. Hadrawi [f,g], Navid Nasajpour-Esfahani [m], Morteza Alizade [h], Majid Zarringhalam [i], Soheil Salahshour [j,k,l], D. Toghraie [n,*]

[a] Shanxi Engineering Vocational College, Taiyuan, Shanxi, 030009, PR China
[b] Department of Petroleum Engineering, Al-Amarah University College, Maysan, Iraq
[c] Department of Nutrition, Cihan University-Erbil, Kurdistan Region, Iraq
[d] Department of Mechanical Engineering, Faculty of Engineering, University of Kufa, Iraq
[e] Nanotechnology and Advanced Materials Research Unit (NAMRU), Faculty of Engineering, University of Kufa, Iraq
[f] Refrigeration and Air-conditioning Technical Engineering Department, College of Technical Engineering, The Islamic University, Najaf, Iraq
[g] Computer Engineering Department, Imam Reza University, Mashhad, Iran
[h] Department of Mechanical Engineering, South Tehran Branch, Islamic Azad University, Tehran, Iran
[i] Young Researchers and Elite Club, South Tehran Branch, Islamic Azad University, Tehran, Iran
[j] Faculty of Engineering and Natural Sciences, Istanbul Okan University, Istanbul, Turkey
[k] Faculty of Engineering and Natural Sciences, Bahcesehir University, Istanbul, Turkey
[l] Department of Computer Science and Mathematics, Lebanese American University, Beirut, Lebanon
[m] Department of Materials Science and Engineering, Georgia Institute of Technology, Atlanta 30332, USA
[n] Department of Mechanical Engineering, Khomeinishahr branch, Islamic Azad University, Khomeinishahr, Iran

ARTICLE INFO

Keywords:
Phase change materials (PCMs)
Heat sink
Thermal management
Heat exchanger
Spiral heat sink

ABSTRACT

Today, every device that a person uses depends on electronic equipment, frequent and long-term use of it causes to heat up and as a result, slow down the speed and performance of that device. In more important and sensitive equipment such as medical equipment, slow speed and reduced performance cause irreparable damage. Therefore, to cool these devices, their internal electronic equipment must be cooled. In studies by others, the simultaneous use of several phase change materials and airflow in the form of layer-by-layer contact was usually less studied. In this study, using CNC machining, a heatsink consisting of 2 spirals was produced. In the first spiral, PCM Paraffin Wax with different volume percentages and in the second spiral, the presence or absence of forced airflow in heat transfer rate 2.9 W to 3.7 W was tested with a step of 0.4 W and the results were that by adding %50 PCM and adding 100 % PCM to the system, its performance increases by 7.19 % and 44.91 %, respectively, which shows using the maximum volume capacity of PCM increases efficiency. Also, by adding forced airflow to the system, its performance has increased by 7.71 %. It can be said that if the forced airflow in the system is used layer by layer, it prevents the heat from concentrating in certain parts of the heatsink and the circuit, which results in the same heating of the whole system and the heat is evenly distributed throughout the heatsink.

1. Introduction

One of the topics that has always attracted the attention of researchers is the topic of heating and cooling in various systems such as electronic equipment, solar collectors, pipes, combustion, heat exchangers, etc [1–5]. The need for continuous and complete use of equipment, in which electronic components are used, is rapid cooling and reaching the allowable temperature in the components. If the equipment used is overheated and cannot transfer the heat generated out of the system, it will cause the system to slow down and eventually reduce efficiency. According to the US Air Force, 55 % of electronic equipment failures are caused by system overheating [6]. Therefore, a lot of research has been done on the cooling of electronic equipment,

* Corresponding authors.
E-mail addresses: raincy930520@163.com (Y. Wang), Toghraee@iaukhsh.ac.ir (D. Toghraie).

https://doi.org/10.1016/j.asej.2024.102793
Received 8 July 2023; Received in revised form 31 January 2024; Accepted 25 March 2024
Available online 4 April 2024
2090-4479/© 2024 THE AUTHORS. Published by Elsevier BV on behalf of Faculty of Engineering, Ain Shams University. This is an open access article under the CC BY-NC-ND license (http://creativecommons.org/licenses/by-nc-nd/4.0/).

Nomenclature

Q	heat transfer rate (W)
V	Voltage (V)
I	Current (A)
m	Mass (gr)
C_p	Specific heat $\left(\frac{kJ}{kg.^{\circ}C}\right)$
T	Temperature (K, °C)
t	Time (S)
H	Latent heat $\left(\frac{kJ}{kg}\right)$
Subscript	
i	Inlet
s	Heat power
a	Air
h	Heat sink
P	Paraffin Wax
ah	Air inside the heatsink

which can be mentioned as follows: thermoelectric coolers [7], spray cooling [8], microchannel cooling [9], immersion cooling [10], extended surface [11], heat pipe [12], piezoelectric pump [13], heat sink with PCM [14] were proposed and used. Another way to cool electronic equipment is to use a spiral heatsink. About using spiral heat sink, Shingo Otake and colleagues proposed a special model of the heatsink with spiral blades, which increases the system efficiency by 14.9 %, regardless of the thickness, number and pitch of the fins [15]. Also, Bahiraei et al. [16] studied a spiral heatsink model numerically, investigated the effect of heatsink material and air velocity on the spiral path, and concluded that the spiral thermal heatsink has a better trend in terms of heat transfer than a normal heatsink goes through. Regarding the capacity and heigh of using PCM in each test, Siyabi et al. [17] examined the system performance under heat transfer rates 1 to 2 W with different volume percentages of PCM and its arrangement and concluded that the maximum volume percentage of PCM causes the system to be at the highest level of performance, and, Alizadeh et al. [18] by examining the height of the PCM inside a particular model of heat sink, conclusion that by adding maximum phase change material to the system, the heating time of the system can be postponed by 49.7 %. Also, the effect of using iron wool in the experiments was investigated by Prieto et al. [19]. They examined the effect of using iron wool to accelerate the heat transfer process and sodium nitrate as a phase change material, using a fabricated sample and concluding that using this method can increase heat transfer from the system to the environment by up to 300 % and at leat the effect of using forced air flow to cooling the system in the test was investigated. Numan et al. [20] examined the effect of using forced air jets when applied to a particular instance of a heatsink, and evaluated the number, height, and dimensions of the heatsink, and concluded that the use of 9 with a height of 33 mm and using airflow, the efficiency of the system has increased by 25.3 %. Khor et al. [21] examined the effect of heat transfer rate and forced airflow on three specific heatsink models with different configurations and found that the results depended on the heat applied to the heatsink, which is strongly dependent on the heatsink design and fluid flow velocity. As the flow rate increases, the cooling of the system increases. By designing a specific type of capsule and filling it with PCM, Dolado et al. [22] evaluated the thermal behavior of single-capsule and double capsule under forced airflow and found that using capsules and forced airflow could increase efficiency by up to 12 % compared to no forced airflow mode. Kalbasi [23] was tested a specific model of heatsink in three modes. In the first stage, he passed air between the blades, and in the second stage, he filled the space between the blades with PCM, and in the third stage, he used it in combination, and all these experiments were tested at a constant heat transfer rate, and he concluded that system efficiency and heat transfer coefficient increase significantly. Anzar et al. examined a specific model of the heatsink. At first, they passed through the air box, then split it in two, applied PCM in the upper half and airflow in the lower half, and then filled the entire box with PCM. They tested the design numerically in both charge and discharge modes [24]. The most important problem with the use of PCMs is their slow cooling and solidification, which has only been used in previous reviews, and it has rarely happened that the cooling and solidification of PCM is also investigated. But in this test, with the simultaneous use of air and PCM, the cooling of the heat sink occurs faster, and the PCM returns to a solid state and ready to work faster after liquefaction.

In this test, a spiral heat sink consisting of two separate paths was designed and built, in one path PCM was used and in the other path, forced air flow was used to cool the heatsink. The presented design is a completely new example and it can be used to cool the heat sink using PCM and air can flow inside the system.

2. Experimental setup

Using special software for mechanical design, a special model with specific dimensions and conditions was designed and then produced by CNC machining. The made heatsink was tested after final control and approval under laboratory conditions and in heat transfer rates 2.9 W to 3.7 W with 0.4 W step (2.9, 3.3 and 3.7 W). Also, this design was tested in the presence or absence of forced airflow and also with different volume percentages of PCMs in laboratory conditions and with specified measurement accuracy.

In this test, the air is passed through a separate path inside the heat sink by the pump and while moving, it cools the heat sink and the PCM located in another separate path. Practically, with this method, both the forced air flow and PCM have been used in order to increase the efficiency of the system.

2.1. Test samples

For experimental studies in the use of PCMs, three different models were used in terms of different volume percentages, i.e., 0 % PCM, 50 % PCM and 100 % PCM. Also, all these conditions were re-examined in the case of no forced airflow and despite the forced airflow. The heatsink designed, on which all the tests were performed, is made of 6061 Aluminum, which is designed, modeled by special software and produced by CNC (computer numerical control machine) machining. Table 1 shows the dimensions of the heatsink used. The material used in this design has thermophysical properties that include melting point, specific heat capacity, thermal conductivity, density, and so on. These properties can also be seen in Table 2.

In terms of the general classification, the performed experiment can be divided into three parts: power source and heat transfer rate control, the part under test and heat source, and the data recording part in the computer. It should be noted that the three sections are presented and announced separately, which can be seen in Fig. 1. The prototype tested is shown in Fig. 1, and in this test, heat transfer rates of 2.9, 3.3, and 3.7 W were used. Because the designed heat sink sample has the ability to transfer heat in this amount of heat transfer rate, and in other words, this heat sink model has the highest efficiency in the applied heat transfer rate range.

Fig. 2 shows all the shapes, designs and assembly methods. As shown

Table 1
Main geometric parameters of the heatsink.

Parameters	Outer Diameter	height	Inner dept	Wall thickness
Value (mm)	$\varnothing = 120$	$H = 15$	$h = 10$	$t = 1$

Table 2
Thermophysical properties of Aluminum 6061.

Parameters	Melting point (°C)	Specific heat capacity C_p (kJ/kgK)	Thermal conductivity k (W/mK)	Density ρ (kg/m^3)
Aluminum	1199	963	180	2730

in Fig. 2-a, the general view of the more design, which is made of Aluminum, is shown. In Fig. 2-b, the general views that were used in this experiment are shown. Fig. 2-a shows the diagram of the heatsink design used, and it should be noted that the outer diameter and overall height of the heatsink are $\varnothing = 120mm$ and $15mm$, respectively.

As shown in the picture, the inside of the heatsink was emptied with the help of CNC and made two separate parts in the form of a spiral that is not in contact with each other in any way. Each of these spiral segments is in a separate path in a spiral path that starts from the center and ends at the farthest point from the center of the circle. The thickness of each spiral path is $5mm$ and the thickness of the meat between the two paths is $1mm$. As shown in the figure, each helical path consists of 4.5 turns so that the starting point of the path and the endpoint of the path are approximately in the same direction. The machining depth in these two spirals is equal to $10mm$, and finally, the remaining thickness of the bottom of the heatsink for heat exchange has reached 5 mm. The upper and lower surface of the heatsink has been machined for integration and smoothing. The desired dimensions of this design can be seen in Table 1.

As shown in Fig. 3-a, the silicone paste is a device that is used to minimize the thermal resistance between surfaces. For this purpose, Fig. 3-b shows that in this experiment, a layer of silicone paste was used between the heat source and the heatsink to remove air between the two

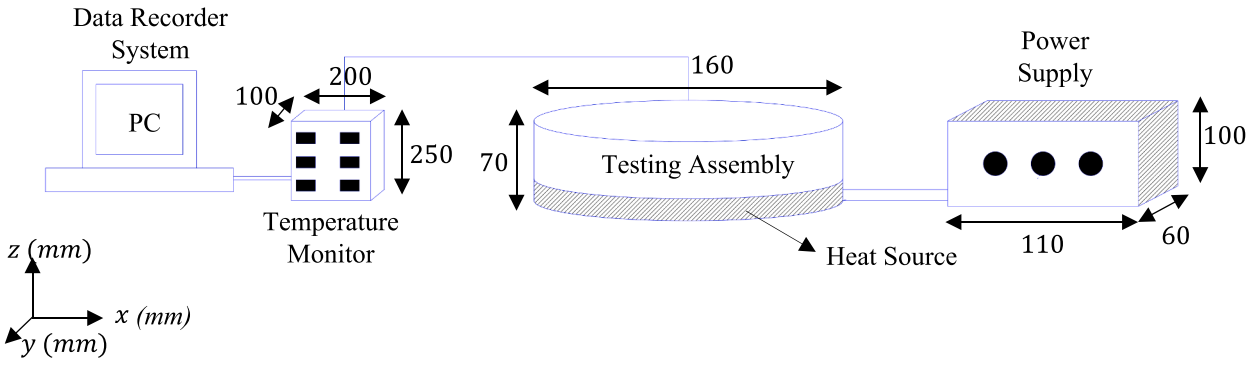

Fig. 1. Schematic diagram of experimental set.

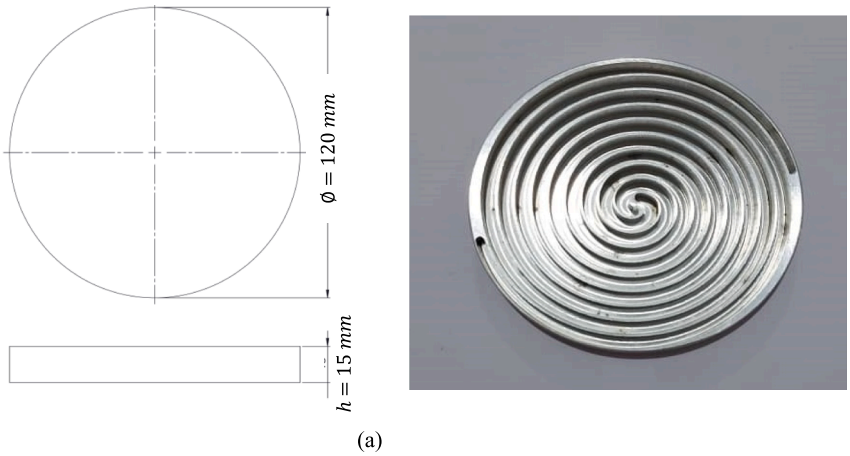

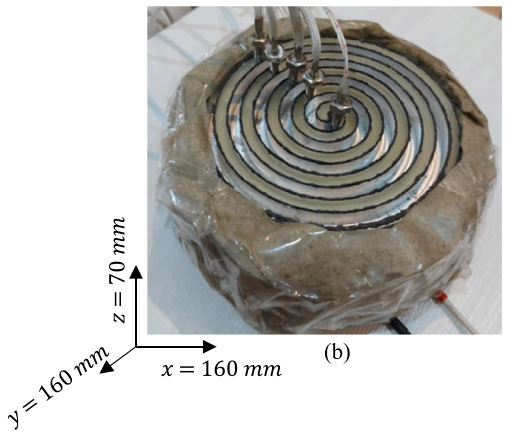

Fig. 2. an overview of the experimentally study set.

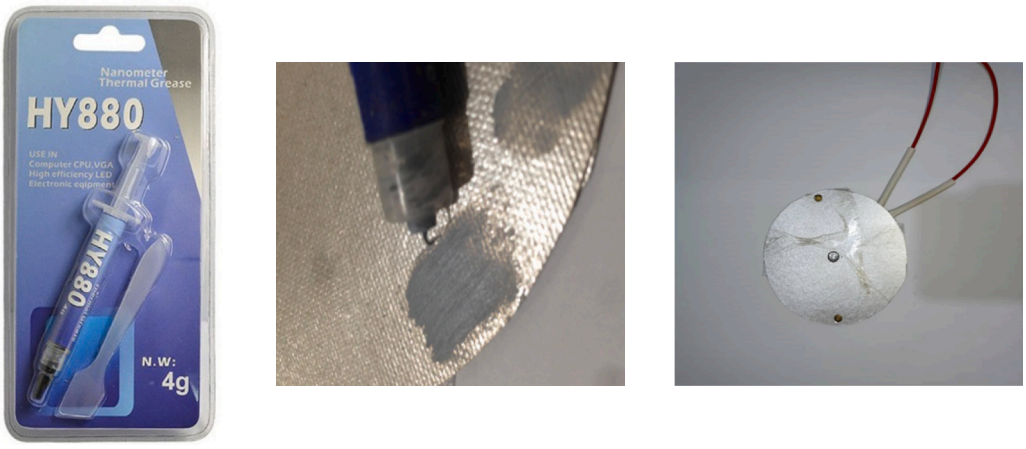

Fig. 3. An overview of the (a) silicone paste, (b) a layer of silicone paste, (c) heat source.

surfaces and minimize thermal resistance. In the industry, screws are used to strengthen the connection of the heatsink to the IC. In this way, a hole is created on the heat sink and the system board with the help of machining operations, and these two parts are connected to each other by screws, of course, before the permanent connection, a layer of silicone paste is used between them.

The heat source used in this experiment is such that it occupies the entire surface of the heat sink, so it can be said that the dimensions of the heat source used are 120 mm in diameter and 20 mm thick, it was shown in Fig. 3-c. Because PCM melts during the phase change and has the possibility of leaking into the surrounding environment, it must be placed in a box. One of the things that can hold the PCM is the aluminum box. On the other hand, in order for the heat sink to be able to absorb the heat produced by the heat source well, the heat sink should be connected to the heat source with the help of glue and silicone paste. As it is clear in the Fig. 3, in this experiment, an alternative heat source of the system IC is used to simulate the heat generated by the IC and it is shown in the silicon paste used in this experiment. As shown in the Fig. 3, a layer of silicone paste is placed between the heat source and the heat sink.

The maximum power produced by the heat source is 150 W. It is directly connected to 220 V AC power and to apply different heat transfer rates inside the path, a dimmer and a potentiometer are used. By rotating the dimmer and reading the numbers entered in the potentiometer, the desired heat transfer rates can be applied to the system. To observe the phase change process of PCMs, a layer of Plexiglass with a thickness of 5 mm and a diameter of 120 mm was used, which is placed on the heatsink, and despite this, the behavior of PCM can be easily observed. Also, since the test conditions should be completely isolated and no heat transfer from the system to the environment or vice versa should occur, the perimeter of the system is covered by a layer of rock wool 50 mm thick and only the top surface of the heatsink is open. It is also controlled with the help of Plexiglas. For the two spirals inside the heatsink not to be in contact with each other from the top, the distance between the heatsink and Plexiglas is covered with sealing glue. With this, the two spirals inside the heatsink are no longer in physical contact with each other, and only the contact between them is in the form of heat transfer between the two spirals.

As summarize it can be said that, in this mechanism the heat generated by the IC is transferred to the heat sink with the help of a layer of silicon paste, and after passing through the aluminum heat sink, it is absorbed by PCM. This happens so that the heat of the electronic system does not exceed the permissible value and its performance is not disturbed.

On the other hand, by passing the forced air flow through a separate path on the side of the PCM, that makes it possible for the Paraffin Wax to melt later and in other words it can absorb more heat from the IC.

2.2. Specifications of PCMs

In this experiment, Paraffin Wax was used as PCM. The melting temperature of Paraffin Wax is between $56-58\ ^{\circ}C$ and the maximum amount of Paraffin Wax used in this experiment was $26 \pm 1gr$. Also, the thermophysical properties of Paraffin Wax can be seen in Table 3. Thermophysical properties include thermal conductivity, specific heat, latent heat, melting temperature, etc.

A SEM image of the pure Paraffin Wax is shown in Fig. 4-a. We can understand that the Paraffin Wax crystallize into randomly oriented micro-platelets with a lamellar inner structure, as it is typical for alkanes with linear molecular structures and long carbon chains. As it is known, this substance is in solid state in the form of crystallized grains and separated from each other. Also, the solid grains of Paraffin Wax can be seen in Fig. 4-b.

2.3. Experimental test rig

Experimental testing Fig. 5 shows the position of each of the thermocouples and also shows the coordinates of each sensors. One of the best sensors that can be used in this test and record temperature changes is K type thermocouple, so in this test, 7 K type thermocouples with a measurement accuracy of $\pm 0.1\ ^{\circ}C$ were used. To measure the temperature between the heat source and the heatsink, because there is no distance between the two and all the space is filled with silicone paste and on the other hand, the heat source is a thin layer. The upper and lower surfaces are not different in temperature from each other, so the number 7 sensor is attached to the lower surface of the heat source to be able to measure the temperature produced by this source. Also, sensor number 1 is used to measure the temperature of the laboratory environment at a distance of $20cm$ from the system and sensor number 2 is used to measure the temperature of the air leaving the heatsink (through the spiral through which the air passes) in the last layer of this spiral and in the farthest the distance is from the center.

To measure the temperature changes of the second helix (the helix in which PCM is), 4 sensors with different special positions were used. As shown in Fig. 5, sensor 3 is located in the earliest ring of this spiral, about $5cm$ from the surface of the heatsink. Also, sensor number 4 is located in the second ring of the spiral inside which is PCM and at a depth of 5 cm from the surface of the heatsink, and sensor number 5 in the third ring and sensor number 6 in the fourth ring (farthest position from the center inside the heat sink) is deployed. It should be noted that sensors 3 to 6 according to Fig. 3 are in one direction with an angle of 80

Table 3
Thermophysical properties of Lauric Acid and Paraffin Wax.

Material	Melting PointT_m(°C)	Latent Heat$\Delta H(kJ/kg)$	Specific Heat Capacity$C_p(kJ/kg.K)$		Thermal Conductivity$k(w/m.K)$		$T_{boiling}$ (°C)	Flash Point (°C)	Density$\rho(kg/m^3)$	
			Solid	Liquid	Solid	Liquid			Solid	Liquid
Paraffin Wax	56–58	173.4	1.92	3.26	0.212	0.167	> 370	> 200	880	790

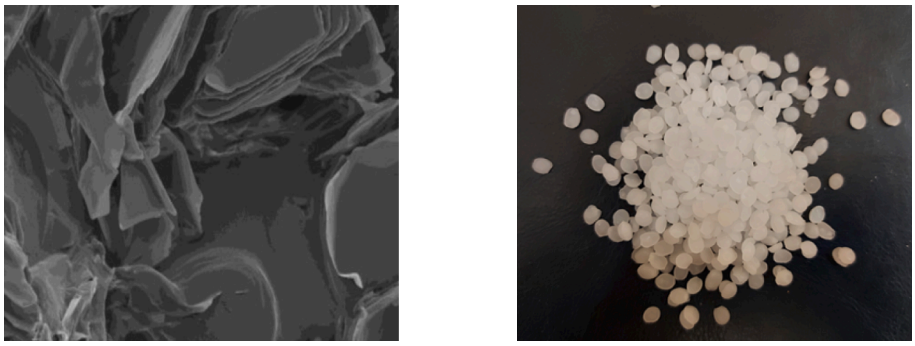

Fig. 4. A view of a) SEM photograph of Paraffin Wax and b) Paraffin Wax used.

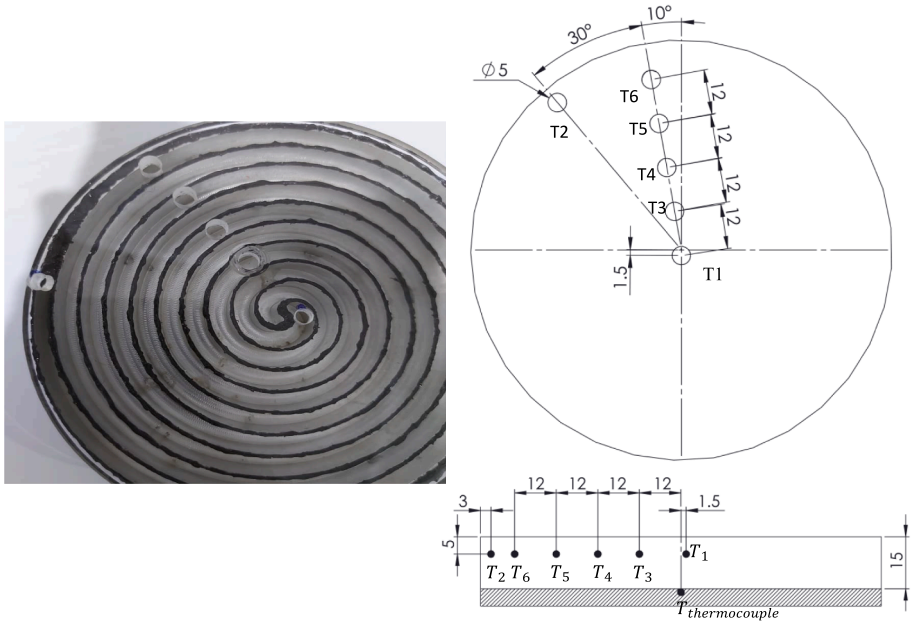

Fig. 5. Thermocouple's situation in the set.

degrees to the horizon and also sensor 2 with an angle of 50 degrees to the horizon. They are connected and placed inside the heatsink in such a way that a nut is assembled on the thermocouple and then in specific parts of the Plexiglass by drills and clamps, the thermocouple is easily assembled on the Plexiglass and the heatsink. The accuracy of the heat source used for the current is ±%0.01 and for the voltage is ±%0.3 at ambient temperature. All tests performed in this experiment were performed at an ambient temperature of 21 °C and an accuracy of 0.3 °C. To validate the performed experiments, each of the tests was repeated 3 times. Regarding the repeatability of the experiment, it can be said that the mismatch was ±%3. Boiling water was also used to calibrate the thermocouples used in this experiment, which showed that the temperature measurement error was less than %0.4.

2.4. Test methodology

In this test, 18 steps were investigated, in the first step, the heat sink did not have a Parrafin Wax and only the heat transfer rate 2.9 W was applied to the system, and the data recording started exactly from the beginning of the heating process, and the test has been done until the system reaches a temperature of 80 °C. Data was also recorded every 20 s. In the second step, the inside of the heat sink did not have the Paraffin Wax, and the test was exactly the same as the first step. With the difference that at this step, as soon as the heating process starts with the help of a fan, the forced flow of air has also been circulated in the system, and the data has been recorded again. Steps 3 and 4 are exactly the same as steps 1 and 2, with the difference that in these steps, heat transfer rate

3.3 W has been applied to the system. Also, steps 5 and 6 were done as before, and this time heat transfer rate 3.7 W was applied to the system and data was recorded.

In the step of 7, the inside of the heat sink is filled up to a height of 4 mm with the Paraffin Wax (50 % of the volume inside the heat sink), and the fan is turned off, and after that the heating process, the test is done, and the test is done until the temperature recorded by the thermocouples reaches 10 degrees above the melting point of the PCM. At this step, a heat transfer rate of 2.9 W was applied to the system. In the step of 8, as in the previous step, the inside of the heat sink is again filled with Paraffin Wax up to a height of 4 mm, and as soon as the heating process starts, the forced air flow is started and continued until the end of the experiment. At this step, a heat transfer rate of 2.9 W was applied to the system. Steps 9 and 10 are exactly the same as steps 7 and 8, with the difference that in these steps, a heat transfer rate of 3.3 W has been applied to the system. Also, steps 11 and 12 were done as before, and this time a heat transfer rate of 3.7 W was applied to the system and data was recorded.

In the step of 13, the inside of the heat sink is filled with PCM up to a height of 8 mm(100 % PCM), and after that, the heat transfer rate application process is started with the help of a heat source, and the test continued until the PCM inside the heatsink was completely melted and reached a temperature of 10 degrees above that. At this stage, a heat transfer rate of 2.9 W was applied to the system. The 14th step is exactly the same as the previous stage, with the difference that as soon as the heating process starts, the fan is also activated and the forced air flow inside the heat sink is rotated. At this step, a heat transfer rate of 2.9 W was applied to the system. Steps 15 and 16 are exactly the same as steps 13 and 14, with the difference that in these steps a heat transfer rate of 3.3 W is applied to the system. Also, steps 17 and 18 were done as before, and this time a heat transfer rate of 3.7 W was applied to the system and the data was recorded.

It should be noted that PCMs change volume after the phase change. For this purpose, in this system, considering that the machining depth of the heatsink is 10 mm and the test was performed at 50 % height and 100 % height, so for filling PCM, the machining depth is assumed to be 8 mm and therefore 50 % of its height is equal 4 mm and 100 % of its height is equal to 8 mm. In general, the amount of PCM consumed in this test at each stage is shown in Table 4. Briefly, the test conditions are shown in Table 5.

2.5. Assumptions

In the experiment that was performed to simplify and according to the necessary measures can be assumed that in this system the ambient temperature is constant and also the transfer of heat from the system to the environment for the use of rock wool has been neglected and in forced currents, constant flow rate was used to transfer air, and after each test, a break was occurred until the system reached full ambient temperature. In this experimental test, the temperature of the air entering the system was 22 °C±0.1 and the flow rate of the air entering the system was 0.05 L per second.

Also, the energy formula of Paraffin Wax can be shown:

$$Q_i = Q_s + Q_a \tag{1}$$

Where Q_i is the input of heat source and the unit of Q_i is Joule, Q_s is the heat of heat power and the unit of Q_s is Joule. Also, Q_a is the heat released from the system by the air and the unit of Q_a is Joule.

$$Q_i = V \times I \tag{2}$$

where V is voltage in Volts and I is current in Amperes, on the other hand, because the first box is insulated with rock wool, it is adiabatic and the Q_a is only through the hot air leaving the system. Q_s is inside the heat sink, which can be written as follows:

$$Q_s = Q_h + Q_P + Q_{ah} \tag{3}$$

where Q_h is the sensible heat absorbed by the heat sink in Kilo Joule (KJ), Q_P is the sensible heat absorbed by Paraffin Wax in Kilo Joule (KJ), Q_{ah} is the heat absorbed by the air inside the heatsink in Kilo Joule (KJ). The volume air of inside the system is small, thus can be ignored.

$$Q_s = m_h C_{p_h} \frac{dT}{dt} + m_L \left(C_{p_L} \frac{dT}{dt} + H \right) \tag{4}$$

where m_h is a mass of the heat sink and the unit of m_h is Kilogram (Kg) and m_P is a mass of the Paraffin Wax in the test was used and the unit of m_p is Kilogram (Kg). C_{p_h} is the specific heat in $\frac{Kj}{Kg^{\circ}C}$ of the case and C_{P_P} is the specific heat of Paraffin Wax in $\frac{Kj}{Kg^{\circ}C}$ and $\frac{dT}{dt}$ is the temperature gradation, H is the latent heat of Paraffin Wax in $\frac{KJ}{Kg}$.

2.6. Validation

In this research, because the presented plan is a completely novel and new idea, it is not possible to use other people's experiments to validate the experiment. For this reason, a reproducibility method was used to refer to these tests, each test was run four times under the same conditions, and the results show a test-to-measurement error rate of less than 0.4 %.

The measurement error is the difference between the approximate value of the product, price and the actual value. Relative error can be calculated as a percentage using the relative error formula.

The mistakes of measuring system are due to the inevitable mistakes of measuring system and the bounds of human eyes. Errors are available distinctive sizes, and you could want to decide if the mistake is so big that the measurements are meaningless. The smaller the mistake, the nearer it's far to the real value.

There are three main types of measurement error:

- Total error

Absolute error is the difference between the measured value and the actual value. The formula for absolute error is:

$$E_{absolute} = \left| X_{measured} - X_{accepted} \right|$$

- Relative error

It expresses the ratio of the absolute measurement error to the allowable measurement error. Relative error can be expressed as:

$$\text{Relative Error} = \frac{|measuredvalue - actualvalue|}{actualvalue}$$

- Percentage Error

Percentage error is similar to relative error, but here the error is converted to a percentage. The formula for percent error is:

$$PercentofError = \frac{|measuredvalue - actualvalue|}{actualvalue \times 100\%}$$

Table 4
PCM consumption at every stage.

Amount of PCM (%)	height (*mm*)	consumption weight (*gr*)	Consumption volume (cm^3)
0	0	0	0
50	4	13	14.4
100	8	26	29

Table 5
Test conditions at each step.

Steps	Step 1	Step 2	Step 3	Step 4	Step 5	Step 6	Step 7	Step 8	Step 9	Step 10	Step 11	Step 12	Step 13	Step 14	Step 15	Step 16	Step 17	Step 18
heat transfer rate (W)	2.9	2.9	3.3	3.3	3.7	3.7	2.9	2.9	3.3	3.3	3.7	3.7	2.9	2.9	3.3	3.3	3.7	3.7
Volume of PCM (%)	0	0	0	0	0	0	50	50	50	50	50	50	100	100	100	100	100	100
forced air flow	×	✓	×	✓	×	✓	×	✓	×	✓	×	✓	×	✓	×	✓	×	✓

3. Result and discussion

3.1. Comparison of temperature sensors without PCM

Because in all tests, sensor number 1 has the task of controlling the ambient temperature and any changes in the system have not affected the environment, so this sensor is not considered for comparison and conclusion. Fig. 6-a shows the temperature changes of sensors T1 to T6 in a state that different temperature sensors were at heat transfer rate of 2.9 W without PCM and forced airflow, and as shown in Figure, the x-

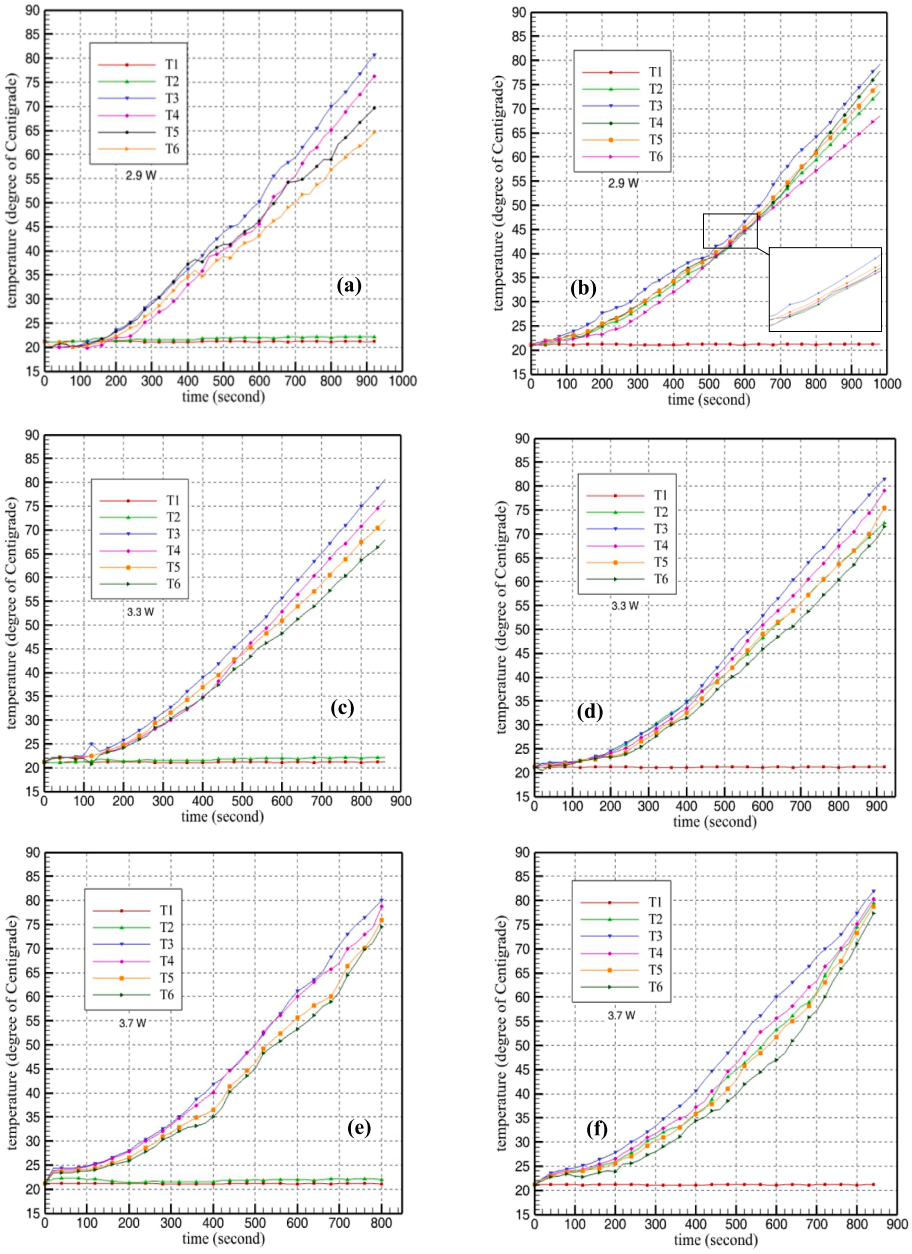

Fig. 6. Temperature variation of thermocouples in melting process at %0 PCM: (a) 2.9 W without air flow, (b) 2.9 W with forced air flow, (c) 3.3 W without air flow, (d) 3.3 W with forced air, (e) 3.7 W without air flow, (f) 3.7 W with forced air.

axis represents the time in seconds from 0 to 1000 s with step 100, and the y-axis represents the temperature in °C from 15 to 90. As it turns out, since the forced airflow is not used at this stage, the T2 sensor is almost constant until the end of the test, and the T3 to T6 sensors, which are in a spiral, respectively, from the center to the outside of that step are cooler because the heat source heats up from the center to the sides. Fig. 6-b shows a situation where a heat transfer rate of 2.9 W is applied and a forced airflow is used. In this case, the growth trend of the sensors is still upward and it can be seen that due to the use of forced airflow, the T2 sensor has an upward growth and after 1000 s has reached the temperature recorded in Fig. 6-a, in other words using current forced air, the system heats 100 s later. Fig. 6-c shows the curve with a heat transfer rate of 3.3 W in the case without PCM and forced airflow. In this diagram, the X-axis represents the time in 0 to 900 s with step 100 s and the Y-axis represents the temperature in terms of Celsius is from 15 to 90 degrees Celsius. Because the applied heat transfer rate is higher than the previous state, the system has reached a temperature of 80 degrees Celsius faster (up to about 850 s). However, in Fig. 6-d, which has a heat transfer rate of 3.3 W without PCM and with forced airflow, the system takes 920 s to reach the maximum temperature and it can be seen in Fig. 6-d that with the addition of forced airflow, the heat is removed from the system and as a result, sensor T2 has increased with increasing time and has reached a maximum of 75 °C. Fig. 6-e shows a heat transfer rate of 3.7 W without PCM and forced airflow. In this case, the X-axis represents the time in seconds from 0 to 800 with a step of 100 s and the Y-axis represents the temperature in °C from 15 to 90 °C. The sensors ascending, record the temperature which shows that the trend of temperature changes is completely ascending, and in this case, the temperatures of T1 and T2 of the system are almost equal to each other. Fig. 6-f, which is related to the same heat transfer rate, with the difference that the forced airflow is used, clearly shows that if the forced airflow is used, the time to reach the maximum temperature is 30 s later, and again the T2 sensor has reached a temperature of 75 °C.

3.2. Comparison of different heat transfer rates in semi-PCM mode

Fig. 7-a shows the temperature changes over time in which Paraffin Wax is used as PCMs and the volume percentage used is 50 %. Also, the

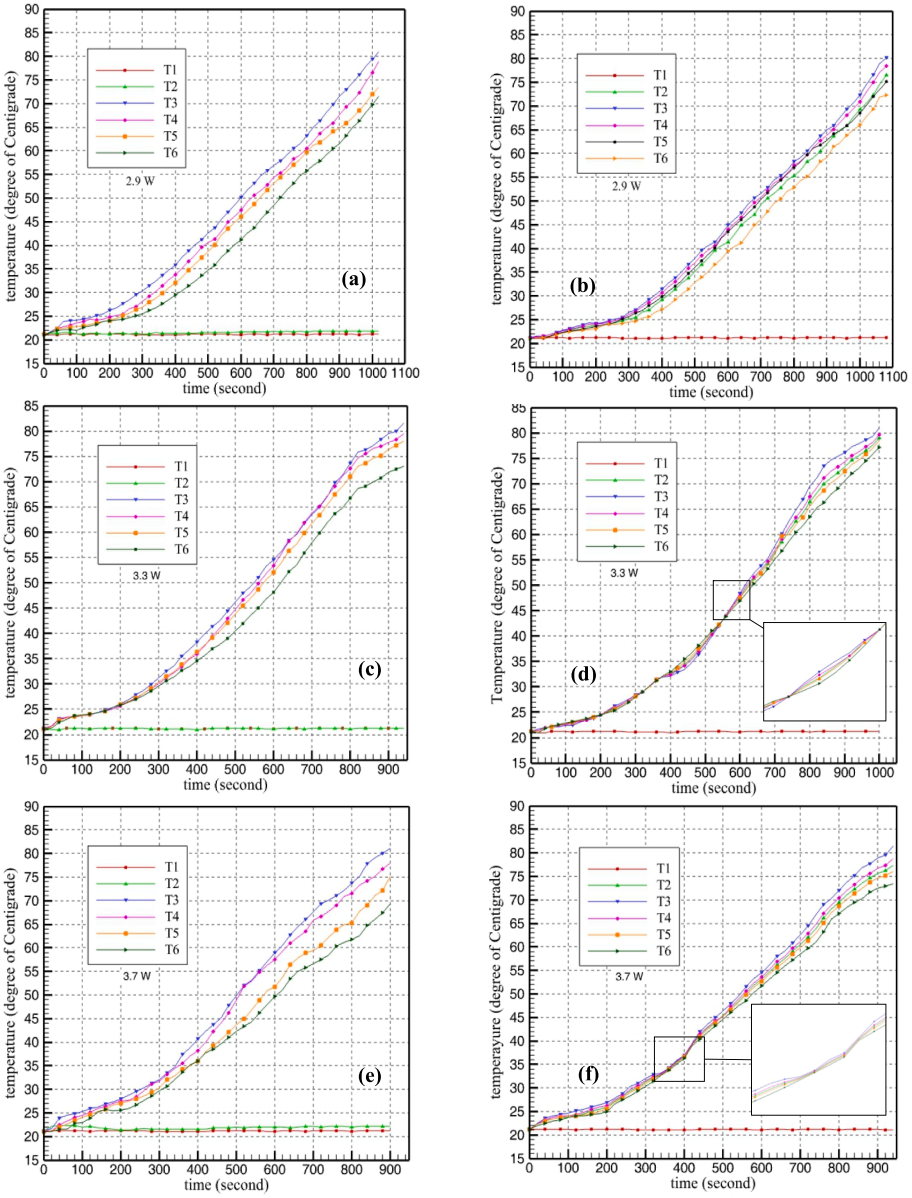

Fig. 7. Temperature variation of thermocouples in melting process at %50 PCM: (a) 2.9 W without air flow, (b) 2.9 W with forced air flow, (c) 3.3 W without air flow, (d) 3.3 W with forced air, (e) 3.7 W without air flow, (f) 3.7 W with forced air.

desired heat transfer rate at this stage is 2.9 W. As can be seen, the X-axis represents the time in seconds from 0 to 1100 s with a step of 100 s and the Y-axis represents the temperature from 15 to 90 °C in steps of 5 degrees. In this case, after about 1020 s, the system reaches the desired temperature (80 °C), and then the test is stopped. According to the previous diagrams, because in the process of charging the system, the heat source is constantly on, so the temperature changes are completely upward, and these changes were more in the center of the system than around. It can be said that the temperatures rises of the sensors occurred with a slope of about 45 %. Fig. 7-b is the same as Fig. 7-a, and each of the axes represents the views mentioned earlier, and the difference in this figure can be said that the presence of forced airflow caused the system to reach the desired temperature 60 s later, and also the T2 sensor accordingly. The previous trend, which had an upward growth in the presence of forced flow, was upward here as well. Can be said that it transfers the heat inside the heatsink to the outside environment because, in the final stages of the test, the output temperature has almost reached the maximum temperature desired by the system. Fig. 7-c shows the state in which the heat transfer rate of 3.3 W is applied to the system and the data recording is done exactly from the beginning. In this diagram, the X-axis represents the time in seconds from 0 to 1000 with a step of 100 and the Y-axis represents the temperature from 15 to 85 with a step of 5 °C. In this heat transfer rate, the time reached the maximum temperature is about 950 s and according to the information obtained from thermocouples, the sensors move up to 800 s, and the temperature range between 65 and 75 °C in a parabolic upward direction and from 800 s later increased linearly. At the most recent recorded time and temperature, the temperature changes between sensors T3 to T6 are in the range of 74 to 80 °C. If forced airflow is used, the data will display other numbers that can be seen in Fig. 7-d. In this diagram, due to the use of forced airflow, this flow helps to distribute the temperature evenly throughout the heatsink. The argument of the issue can be seen in the diagram that after finishing the work, the recorded temperature changes between the T3 to T6 sensors are in the range between 77 and 80 °C. In this diagram, it can be seen that the data recorded by the sensors, finally shows a special curve that can be due to the presence of PCM. Fig. 7-e shows the heat transfer rate of 3.7 W applied to the system in semi-PCM mode with no forced airflow. In this diagram, the X-axis represents the

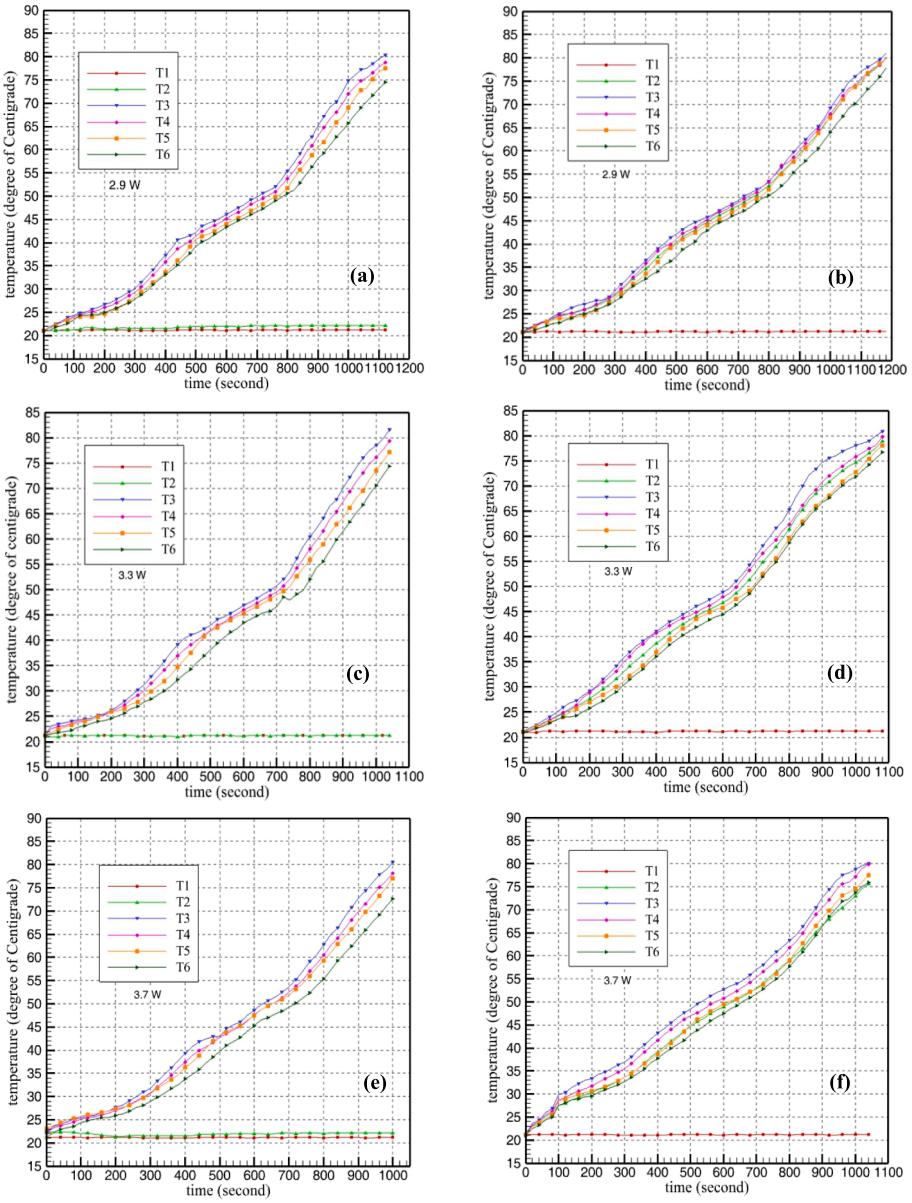

Fig. 8. Temperature variation of thermocouples in melting process at %100 PCM: (a) 2.9 W without air flow, (b) 2.9 W with forced air flow, (c) 3.3 W without air flow, (d) 3.3 W with forced air, (e) 3.7 W without air flow, (f) 3.7 W with forced air.

time in seconds from 0 to 900 with a step of 100 and the Y-axis represents the temperature in degrees Celsius from 15 to 90 degrees Celsius with a step of 5 degrees Celsius. In this diagram, the curve between the sensors is obvious and also after 900 s, the temperature change range between sensors T3 to T6 is from 70 to 80 °C and sensors T2 and T1 are almost equal and move in the same direction. But in Fig. 7-f, the range of temperature changes shown between sensors T3 to T6 is from 75 to 80 °C, and also the temperature of sensor T2 has finally reached 78° C. In this diagram, the X-axis shows the time and the Y-axis the temperature, and after 940 s it reaches the maximum temperature.

3.3. Comparison of different heat transfer rates in Full-PCM mode

Fig. 8-a shows the temperature changes of sensors T1 to T6 at a heat transfer rate of 2.9 W so that there is no forced airflow. In this diagram, the X-axis represents the time in seconds from 0 to 1200 with a step of 100 and the Y-axis represents the temperature in degrees Celsius from 15 to 90 degrees Celsius with a step of 5 degrees Celsius. In this case, considering that the amount of PCM in the system is at its maximum value, so we can observe the behavior of PCM process change in the curve, which is the phase change of PCM from 500 to 800 s in the temperature range of 40 to 50 °C, and finally, after 1120 s, the temperature range of T3 to T6 sensors reaches 75 to 80 °C. Fig. 8-b, which shows the heat transfer rate of 2.9 W and the use of forced airflow, shows the temperature changes of 6 sensors, which are shown in a graph with the X-axis of time and the Y-axis of temperature. The presence of forced airflow at this stage reduces the range of temperature changes of the sensors at the last time from 5 degrees to 3 degrees and this shows that the existence of forced airflow has caused the whole system to show almost the same temperature changes. Also, in this diagram in the time interval of 480 s to 800 s and the temperature interval of 40 to 50 °C, the behavior change zone of PCM is clearly shown and finally, the output temperature (sensor T2) has reached 80 °C and also, to reach the maximum temperature, 1180 s must be spent in this system. The temperature changes of the system for heat transfer rate of 3.3 W without forced airflow and in PCM 100 % can be seen in Fig. 8-c. In this diagram, the X-axis represents the time in seconds from 0 to 1100 with a step of 100 and the Y-axis represents the temperature from 15 to 85 °C with a step of 5 °C. In this diagram, from 500 to 800 s, the PCM begins to phase change and liquefy, and before 500 s, the PCM is taking heat from the system until it reaches the melting point, and after 800 s, the PCM is in the liquid state, is taking heat from the system. Also, the last second temperature range between T3 to T6 sensors is from 74 to 80 °C. Fig. 8-d shows the temperature changes when a heat transfer rate of 3.3 W is applied to the system and assisted by forced airflow. In this diagram, the X-axis represents the time in seconds from 0 to 1100 with a step of 100 and the Y-axis represents the temperature in degrees Celsius from 15 to 85 °C with a step of 5 degrees Celsius. Phase change process of Paraffin Wax occurs in the period of 500 to 700 s and due to the use of forced airflow after reaching the maximum temperature, the temperature difference between sensors T6 and T3 has reached 3 °C and sensor T2 eventually reaches a temperature of 78 °C. Fig. 8-e shows the heat transfer rate of 3.7 W without forced air flow applied to the system. In this diagram, the X-axis represents the time in seconds from 0 to 1000 with a step of 100 and the Y-axis represents the temperature in degrees Celsius from 15 to 90 °C with a step of 5 °C. In this diagram, the phase change phase of PCM has occurred in the time range of 450 to 700 s and the temperature difference between the highest and lowest temperature at the last moment is equal to 7 °C and the temperature trend is still positive and upward and increasing. But in Fig. 8-f, which is accompanied by the same heat transfer rate and this time with forced airflow, the temperature difference between the T3 to T6 sensors at the last time of the test is 4° C and also the PCM phase change interval from 450 to 750 s. In this diagram, the temperature of T2 has reached 75 °C at the end of the experiment, and the course of temperature changes was completely upward, and finally, after about 1030 s it has reached a maximum temperature of 80 °C.

3.4. Comparison of system temperature at a given time with the presence and absence of forced airflow

Fig. 9a shows a bar graph showing a heat transfer rate of 3.7 W and at a fixed time of 800 s, with the X-axis showing the T3 to T6 sensors in both the presence and absence of forced airflow and the Y-axis indicates the temperature in °C from 0 to 85 °C with a step of 5 °C. In this diagram, it is clear that in all sensors, if PCM is not used in the system, the system will reach the maximum temperature faster, and if the system is full of 50 % PCM, it will record a lower temperature at the specified time, and finally use the maximum volume percentage of PCM can show a much lower temperature at a specified time.

Fig. 9b shows a comparison diagram in which the system is subjected to a heat transfer rate of 3.3 W and at a fixed time of 800 s, the diagram is plotted in such a way that the X-axis represents the temperature of the winds without PCM and different volumetric percentages of it, and the Y-axis represents the temperature in degrees Celsius from 0 to 85 °C with step 5. In this diagram, in the case without PCM and 50 % PCM, the conditions are almost equal, but in the case of 100 % PCM at a certain time, the system reaches a lower temperature. Fig. 9c shows a comparison of the sensors in a situation where the applied heat transfer rate is 2.9 W. In this diagram, the X-axis represents the specific temperature of the sensors in different states and the Y-axis represents the temperature. In this diagram, the effect of the presence or absence of PCM can be easily seen, and on the other hand, it shows that by using forced air jets, the system performance will increase. In this curve, in the case without PCM and 100 % PCM, a change of about 10 °C can be observed, and in the case of using forced airflow, this change reaches about 12 °C.

At a heat transfer rate of 3.7 W, mode A is assumed to be 0 % PCM, mode B is assumed to be 50 % PCM, and mode C is assumed to be 100 % PCM. Therefore, in the case with and without forced airflow, the amount of increase or decrease in system performance is specified in Table 6.

Also, at a heat transfer rate of 3.3 W, can be called A) without PCM, B) with 50 % PCM, and C) with 100 % PCM. Therefore, process A to B and process A to C were observed in the case without forced airflow and with forced airflow in Table 7. As can be seen, in the absence of forced

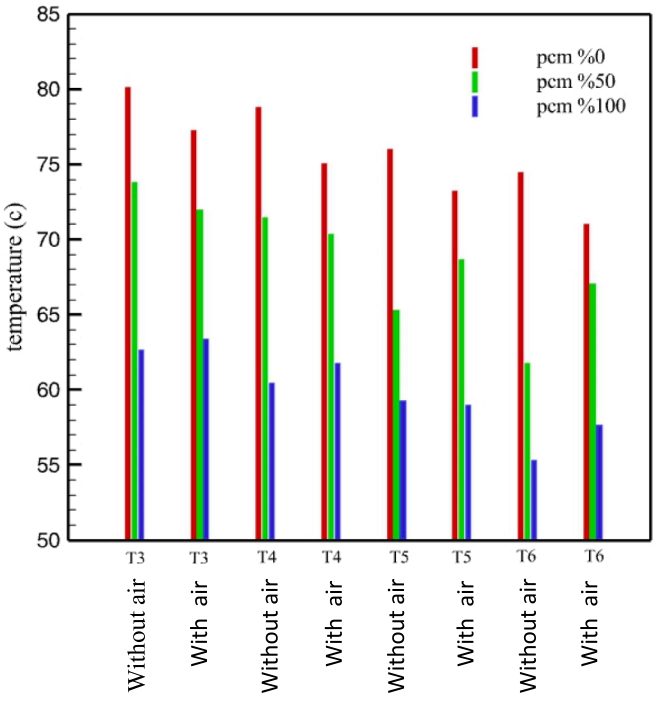

Fig. 9a. bar graph of a heat transfer rate of 3.7 W and at a fixed time of 800 s.

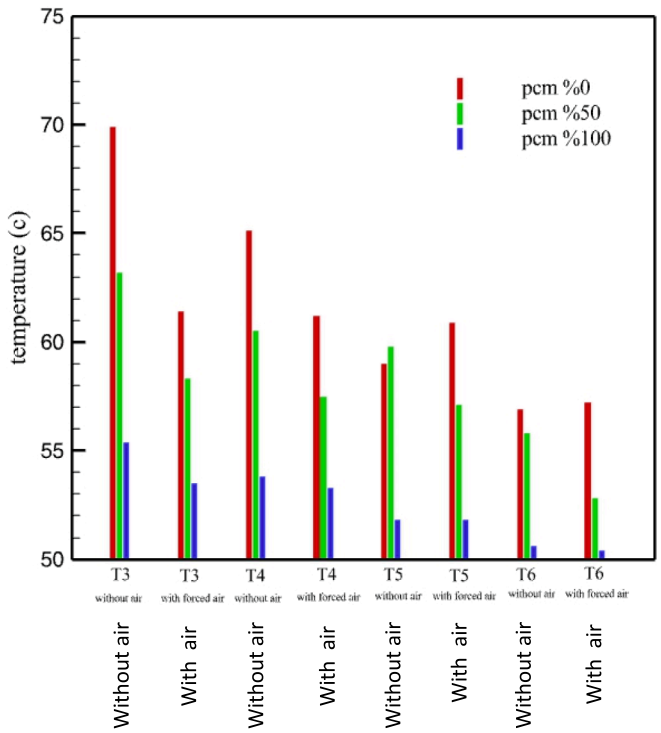

Fig. 9b. bar graph of a heat transfer rate of 3.3 W and at a fixed time of 800 s.

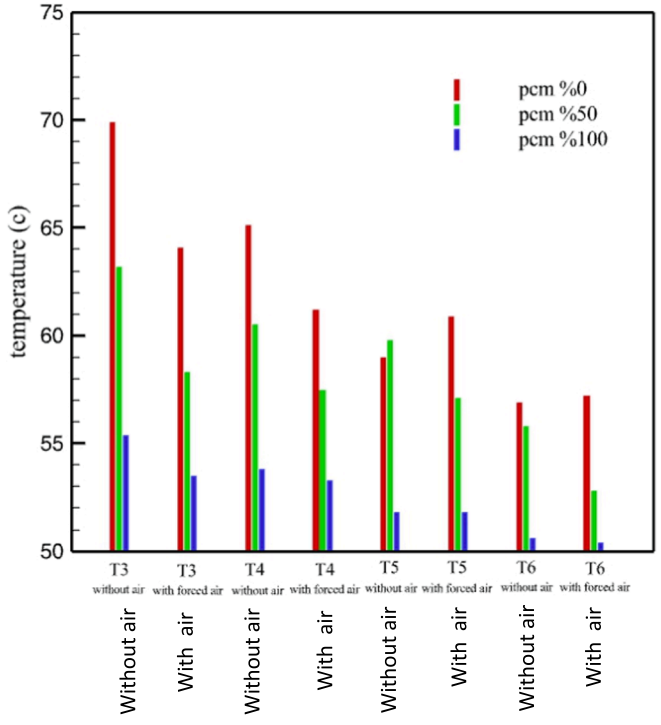

Fig. 9c. bar graph of a heat transfer rate of 2.9 W and at a fixed time of 800 s.

airflow, the progress of the T2 sensor is zero.

Table 8 shows the progress of the system performance in the case without forced airflow and with forced airflow in the case where a heat transfer rate of 2.9 W is applied to the system. According to Table 1, model A) is for when the system has no PCM, mode B) is for when the system contains 50 % PCM, and mode C) is for when the system contains 100 % PCM.

Table 6
comparison of system efficiency at 3.7 W.

Sensors	$A \rightarrow B$(%) without air	$A \rightarrow B$(%) with air	$A \rightarrow C$(%) without air	$A \rightarrow C$(%) with air
T1	0	0	0	0
T2	0	13.1	0	23.3
T3	9.9	11.2	19.6	21
T4	12	12.5	20.7	19.7
T5	12	13.7	18.9	20.6
T6	17.2	15.2	21.9	20.6

Table 7
comparison of system efficiency at 3.3 W.

Sensors	$A \rightarrow B$(%) without air	$A \rightarrow B$(%) with air	$A \rightarrow C$(%) without air	$A \rightarrow C$(%) with air
T1	0	0	0	0
T2	0	1	0	8.8
T3	7.5	8.6	16.4	15.4
T4	4.7	7.3	14.1	14.1
T5	1	4.3	11.6	11.9
T6	1.5	1	9.5	9.6

Table 8
comparison of system efficiency at 2.9 W.

Sensors	$A \rightarrow B$(%) without air	$A \rightarrow B$(%) with air	$A \rightarrow C$(%) without air	$A \rightarrow C$(%) with air
T1	0	0	0	0
T2	0	5.6	0	9.8
T3	9.4	8.2	18.1	15.2
T4	7.5	8.6	15.1	14.6
T5	2.1	9.5	8.5	11.9
T6	1.5	4.2	5.3	5.6

4. Conclusion

This experimental test consisted of a spiral heat sink with two separate paths, which was investigated under heat transfer rates of 2.9 to 3.7 W with a step of 0.4 in different volume percentages of Paraffin Wax, which showed:

- In the first part, the presence or absence of forced air flow in the case that the system does not have PCM can increase the efficiency of the system by 4.9 %. The reason for that is the almost identical temperature of the entire heat sink due to the forced air circulation inside it, and also the transfer of heated air from the system to the surrounding environment.
- In the second part, in the case where the heat sink is filled up to 50 % of PCM and there is no forced air flow, compared to the case without PCM, the system efficiency has increased by 7.2 %, and in the case where forced air flow is used at this stage, the efficiency of the system has increased by 8.2 % compared to the case without PCM and with forced air flow. The reason for that is the property of latent heat capacity in PCM, which has been able to absorb the heat produced by the system. On the other hand, the presence of forced flow has prevented the concentration of heat in a specific area of the heat sink.
- In the third part, when the heat sink is filled up to 100 % with Paraffin Wax, compared to the first part and without forced air flow, the efficiency of the system has increased to 12.5 %, and in the case with forced air flow, its efficiency has increased to 15.3 %

In general, it can be said that:

- If the state without PCM is considered zero, by adding 50 % PCM to the system, its performance will increase by 7.19 % and by adding 100 % PCM to the system, its performance will

increase by 44.91 %, which indicates the existence of PCM, has a great effect on the performance of the system.
- If the state without forced airflow is considered zero, with the addition of forced airflow, the system performance will increase by 7.71 %.
- The presence of a forced airflow prevents the heat from concentrating at a specific point in the heatsink.

On the other hand, it can be said that when the PCM is solid, no natural convection occurs in it, but as soon as this material starts to melt, the heat transfer starts by convection and the heat absorbed from the heat source is transferred to the surface. The top of the heat sink transfers and the result of this event will be the increase of system efficiency.

Declaration of competing interest

The authors declare that they have no known competing financial interests or personal relationships that could have appeared to influence the work reported in this paper.

Acknowledgements

This work was supported by: The first batch of national vocational education teachers' teaching innovation team project of Ministry of Education (YB2020010302). The 14th five year plan of Educational Science in Shanxi Province (GH-220451)

References

[1] Cerin ELDO, Riya K, Mohamed Anees S, rajiniganth E. Treatment of textile plant effluent by using a heat exchanger. International Journal of Communication and Computer Technologies 2019;7(Supplement 1):27–9. https://doi.org/10.31838/ijccts/07.SP01.06.
[2] Jafar Laame G, Rahimy W, Yerel Kandemir S, Acikkalp E. Assessment of greenhouse heating/cooling via heat pump for herat-afghanistan. Renewable Energy Research and Applications 2021;2(1):129–35.
[3] M Sultan, S., Tso, C. P., & M N, E. E. (2020). A case study on effect of inclination angle on performance of photovoltaic solar thermal collector in forced fluid mode, *Renewable Energy Research and Applications. 1*(2) 187-196.
[4] Huang Z, Li T, Huang K, Ke H, Lin M, Wang Q. Predictions of flow and temperature fields in a T-junction based on dynamic mode decomposition and deep learning. Energy 2022;261:125228. https://doi.org/10.1016/j.energy.2022.125228.
[5] Feng X, Jiang L, Li D, Tian S, Zhu X, Wang H, Li K. Progress and key challenges in catalytic combustion of lean methane. Journal of Energy Chemistry 2022;75:173–215. https://doi.org/10.1016/j.jechem.2022.08.001.
[6] U. Soupremanien, H. Szambolics, S. Quenard, P. Bouchut, M. Roumanie, R. Bottazzini, N. Dunoyer, Integration of metallic phase change material in power electronics. In Thermal and Thermomechanical Phenomena in Electronic Systems, IEEE Intersociety Conference, 15th (2016), 125-133.
[7] J.W. Vandersande, J. Fleurial, Thermal Management of Power Electronics using Thermoelectric Coolers, In Proceedings of the Fifteenth International Conference on Thermoelectric, Pasadena, (1996), 26-39.
[8] Lin L, Ronnappan R. Heat transfer characteristics of spray cooling in a closed loop. Heat Mass Transfer 2003;46(20):3737–46.
[9] Koo JM, Im S, Jiang L, Goodson KE. Integrated microchannel cooling for three-dimensional electronic circuit architectures. J Heat Transfer 2005;127(1):49–58.
[10] Zhu L, Boehm RF, Wang Y, Halford C, Sun Y. Water immersion cooling of PV cells in a high concentration system. Sol Energy Mater 2011;95:538–45.
[11] Jaworski M. Thermal performance of heat spreader for electronics cooling with incorporated phase change material. Appl Therm Eng 2012;35:212–9.
[12] Liu XD, Chen YP, Shi MH. Dynamic performance analysis on start-up of closed-loop pulsating heat pipes (CLPHPs). Int J Therm Sci 2013;65:224–33.
[13] Kheirabadi AC, Groulx D. Cooling of server electronics: a design review of existing technology. Appl Therm Eng 2016;105:622–38.
[14] Ashraf MJ, Ali HM, Usman H, Arshad A. Experimental passive electronics cooling: Parametric investigation of pin-fin geometries and efficient phase change materials. Int J Heat Mass Transfer 2017;115:251–63.
[15] Otake S, Tateishi Y, Gohara H, Kato R, Ikeda Y, Parque V, et al. Heatsink design using spiral-fins considering additive manufacturing, IEEE Xplore. International Conference 2019.
[16] Bahiraei M, Mazaheri N. Using spiral channels for intensification of cooling process in an innovative liquid block operated with a biologically produced nanofluid: First and second law analyses. Chem Eng Process - Process Intesif 2021;162:108326.
[17] Al I, Siyabi S, Khanna T, Mallick SS. Multiple phase change material (PCM) configuration for PCM-based heat sinks - an experimental study. Energies 2018;11(7).
[18] Alizade M, Ashtiani HAD, Toghraie D. Experimental study on the effects of different phase change materials for increasing the cooling rate of industrial electronic systems by using a heat exchanger with the specific heat sink. J Storage Mater 2022;55.
[19] Prieto C, Rubio C, Cabeza LF. New phase change material storage concept including metal wool as heat transfer enhancement method for solar heat use in industry. J Storage Mater 2021;33:101926.
[20] H. Numan, S. Muftooh ur Rehman, T. Muhammad, Thermal analysis and optimization of L-shape fin heat sink under natural convection using ANOVA and Taguchi, Thermal Science 2021 First Issue 00, 317.
[21] Khor CY, Rosli MU, Nawi MAM, Kee WC, Ramdan D. Influence of inlet velocity and heat flux on the thermal characteristic of various heat sink designs using CFD analysis. J Phys Conf Ser 2021.
[22] Dolado P, Lazaro A, Marin JM, Zalba B. Characterization of melting and solidification in a real scale PCM-air heat exchanger: Numerical model and experimental validation. Energ Conver Manage 2011;52:1890–907.
[23] Kalbasi R. Introducing a novel heat sink comprising PCM and air-Adapted to electronic device thermal management. Int J Heat Mass Transfer 2021;169(120914).
[24] Anzar A, Shine K. Transient thermal analysis of phase change material based heat sinks, nternational Journal of Research. Eng Technol 2013.